




Synthesis of waterborne polyurethane aerogels-like materials via freeze-drying: an innovative approach

Darío Cantero¹, Esther Pinilla-Peñalver¹, Amaya Romero¹, and Luz Sánchez-Silva^{1,*} 

¹Department of Chemical Engineering, University of Castilla-La Mancha, Avda. Camilo José Cela 12, 13071 Ciudad Real, Spain

Received: 4 March 2023

Accepted: 8 May 2023

Published online:

23 May 2023

© The Author(s) 2023

ABSTRACT

Waterborne polyurethane (WBPUR) aerogels using acetone method and freeze-drying procedure have been successfully synthesized. The morphology, chemical structure, and thermal and mechanical properties of obtained aerogels were analysed by means of scanning electron microscopy, Fourier-transform infrared spectroscopy, contact angle, thermogravimetric analysis, differential scanning calorimetry and dynamic mechanical analysis. In addition, the influence of the solids content in the hydrogel (2–15 wt.%), obtained by varying the amount of water added in the suspension, on the density and thermal conductivity was evaluated. Obtained results demonstrated that the properties of aerogels strongly depend on the solids content assayed in the parent solution. As the solids content in the WBPUR aerogels increases, the density and thermal conductivity for materials with 2.5 and 10% solids content follow an upward trend, while their elasticity decreases. Materials with solids content below 2.5% and above 10% have not demonstrated adequate processability due to their high deformity and hardness, respectively. The drying methodology (freeze-drying) can be profitably used to prepare aerogels-like materials in a cost-effective way.

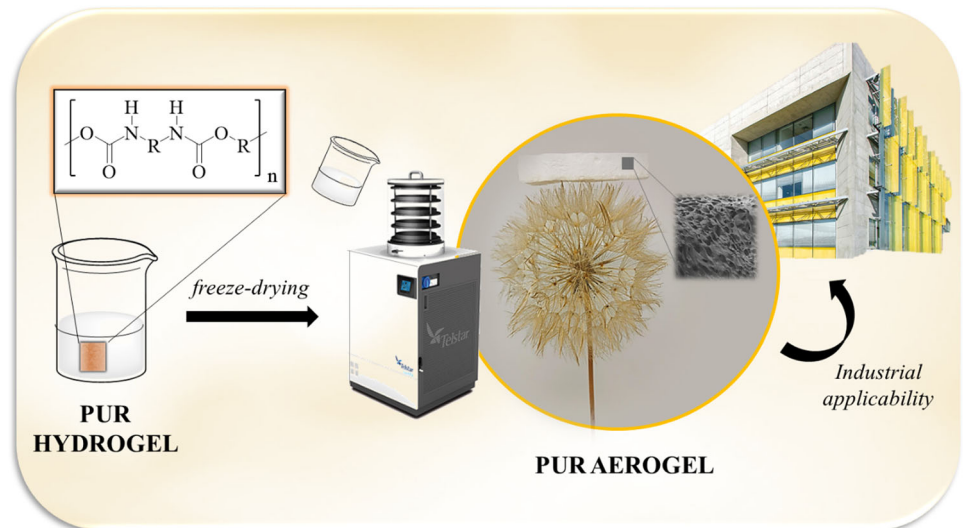
Handling Editor: Maude Jimenez.

Address correspondence to E-mail: marialuz.sanchez@uclm.es

<https://doi.org/10.1007/s10853-023-08579-0>

GRAPHICAL ABSTRACT

Illustration of the alternative preparation process of WBPUR aerogels and its potential industrial application.



Introduction

The current energy situation and the oil crisis generated in recent times have increased concern and awareness about energy saving around the world. In this sense, one of the crucial points to achieve these savings is the correct insulation of buildings, reducing the conditioning needs to maintain the optimum temperature inside. The past studies suggest that estimated energy consumption in the building sector alone could reach 35–40% of the total energy consumed [1], being also the largest greenhouse gas producer [2]. In this context, aerogels appear as very light insulating materials, ideal for fulfilling this mission without compromising the structure of the insulated buildings. Aerogels are predominantly mesoporous solid materials, characterized by a very low density and high porosity, with a large surface area and low thermal conductivity [3–7]. Due to their physical and chemical characteristics, these materials have excellent properties for various industrial applications, such as thermal and acoustic insulation in the construction sector, both in exterior and

interior walls and floors, catalysts, oil spill clean-up agents, or CO₂ capture agents, among others [8–12].

Aerogels can be prepared from different materials, such as silica, polyurethane, polyurea, polyimide, biopolymers, graphene, carbon nanotubes, various metals, and their derivatives [5, 13–18] and can be divided in 4 major groups: inorganic, organic, carbon and hybrid aerogels. *Inorganic* aerogels are based over metal or semi-metallic oxide structures, including silica aerogels, which are the most researched to date and the best insulators at ambient pressure [6, 15, 16]. *Organic* aerogels stand out for having structures based on organic polymers and usually have better mechanical properties than inorganic ones. In addition, their physical characteristics can be adapted by making small changes in the proportions of the reagents used during the synthesis of the materials [19, 20]. *Carbon* aerogels consist of porous materials obtained by carbonizing organic aerogels prepared by the sol–gel method [21]. Finally, *hybrid* aerogels are obtained by combining two of the previously mentioned types of aerogels, with the aim of mitigating the disadvantages of *organic* and *inorganic* aerogels when used separately [22]. Because their

thermal conductivity is lower than that of air, achieved due to the small pore sizes of the material, many of these aerogels can be used in industry as thermal superinsulators. As for the solid phase, the conductivity is limited by the nanostructure and tortuosity of the aerogel structure, as well as by the low solid fraction that these types of materials usually have.

Among the *organic* aerogels, there are different types depending on the polymer used for their synthesis. The first *organic* aerogel was produced from resorcinol–formaldehyde and melamine–formaldehyde [23] and nowadays are used as thermal insulators or adsorbents [24]. Within this group, polyurethane aerogels have been the focus of research and scientific study in recent years [25] due to their excellent properties and multiple applications. As a result of the improvements achieved with these materials throughout history [26–30], materials with very low thermal conductivities and densities have been achieved [22, 31].

Polyurethane aerogels were first obtained by Imperial Chemical Industries (ICI) in 1996, with some good results regarding density ($0.05\text{--}0.15\text{ g cm}^{-3}$) and thermal conductivity ($0.02\text{ W m}^{-1}\text{ K}^{-1}$) [3]. Then, Biesmans et al. [26] discovered the influence of heat treatment on the subsequent physical properties of the aerogel. Diascorn et al. [25] proposed a two-step synthesis, achieving aerogels with very low thermal conductivities ($0.017\text{ W m}^{-1}\text{ K}^{-1}$). Hye-Jin Yoo et al. [27], firstly, observed the chemical structure of these materials, while Teymouri et al. [28] implemented doping with carbon nanotubes, obtaining materials with densities between 0.18 and 1.17 g cm^{-3} .

Sol–gel is one of the most used methodologies to synthesize polyurethane aerogel, forming a colloidal suspension [4, 30]. This suspension forms the final gel after generating a three-dimensional lattice by interlacing the polymer chains. During the sol–gel transition, the bonds formed by Van der Waals forces and hydrogen bonds cause a continuous drastic change from the liquid phase of the solution to a solid phase [30]. Specifically, different polyurethane aerogels were synthesized using acetone as organic solvent, following a procedure known as the acetone method, thus achieving a simple and environmentally friendly synthesis procedure [32–34]. In this work, acetone method was used to produce polyurethane hydrogels and the water contained was removed using freeze-drying. This drying method consumes less resources

during drying [4, 30, 35]. However, there are few works using this methodology to produce polyurethane aerogels.

In addition, the properties of the aerogels were analysed in detail to determinate their physicochemical properties (density, thermal conductivity, mechanical behaviour, porosity, hydrophilicity, thermal stability). Finally, the influence of wt.% solids content (depending on the water content addition) was evaluated on the final properties of polyurethane aerogels obtained to select the most suitable for future industrial applications, such as the insulation for buildings mentioned before, or as a thermal insulator for the aerospace industry, among others.

Experimental

Chemicals

WBPUR aerogel synthesis: Polyethylene glycol [PEG, number-average molecular weight (M_n) = 2000 g mol^{-1} , Sigma-Aldrich]; 2,2-bis(hydroxymethyl)propionic acid [DMPA, 98%; Aldrich Chemicals]; 1-methyl-2-pyrrolidinone anhydrous [NMP, 99.5%, Sigma-Aldrich]; dibutyltin dilaurate [DBTDL, 95%, Aldrich Chemicals]; 4,4'-methylenebis(cyclohexyl isocyanate) [HMDI, 90% mixture of isomers, Sigma-Aldrich]; ethylenediamine [EDA, $\geq 99\%$, Sigma-Aldrich]; triethylamine [TEA, $\geq 99\%$, Sigma-Aldrich]; acetone [HPLC grade, Labkem]. Water was purified by distillation followed by deionization using ion-exchange resins. PEG and DMPA were dried at $60\text{ }^\circ\text{C}$ under vacuum overnight before use. To remove any traces of water in acetone, molecular sieves [3 Å; Sigma-Aldrich] were introduced to an acetone container a few days prior to using it in the synthesis of the polyurethane dispersions. Other solvents and chemicals were used as received unless stated.

Titration and standardizations: dibutylamine [$\geq 99.9\%$, Sigma-Aldrich], toluene [$\geq 99.7\%$, Sigma-Aldrich], bromophenol blue ACS reagent, Sigma-Aldrich], ethanol [99.5%, PanReac], methanol [99.8%, Sigma-Aldrich], hydrochloric acid [ACS reagent, Sigma-Aldrich], potassium hydrogen phthalate [$\geq 99.9\%$, Sigma-Aldrich], sodium hydroxide [98%, Sigma-Aldrich], phenolphthalein [1% ethanolic solution, Sigma-Aldrich], methyl orange [85%, Sigma-Aldrich].

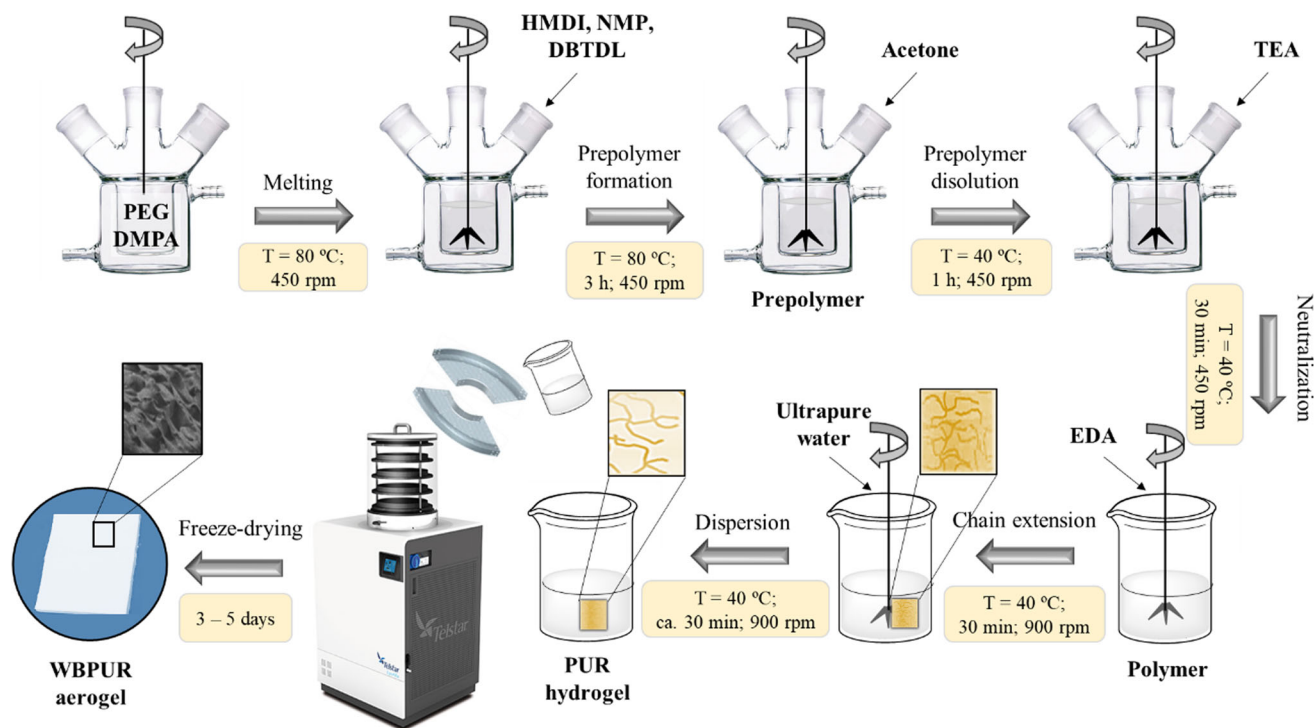


Figure 1 Schematic illustration of the preparation process to synthesize WBPUR aerogels.

Synthesis of waterborne polyurethane aerogels

In this study, waterborne polyurethane aerogels (WBPUR aerogels) were synthesized following the schematic process shown in Fig. 1 and Fig. S1. The synthesis procedure was adapted from the study carried out by Chidambareswarapattar et al. [36]. Here, PEG was used as polyol, HMDI as isocyanate, NMP as anhydrous solvent, DMPA as ionic emulsifier agent, DBTDL as catalyst, acetone as organic solvent, TEA as neutralizer agent, EDA as chain extender, and purified water as dispersion medium for the formed polyurethane. Table 1 shows the proportion of reagents used during the development of the synthesis procedure of the WBPUR aerogels. As can be seen from this summary table, the isocyanate index (R) was 1.5 (mol mol^{-1}). NCO content at different reaction times during the synthesis

process was previously determined as in the previous literature [37], following the UNE-EN 1242:2013 statement hoping to find a low isocyanate content [38]. This evaluation was followed by titration and FT-IR experiments (Fig. S2), being very concordant between both. Thus, before the addition of the chain extender, around 5 wt.% of free isocyanate moieties would remain to start the polymerization.

First, PEG and DMPA (previously dried at 60 °C under vacuum overnight) are melted under mechanical stirring at 80 °C. Once these reagents are melted, HMDI, NMP and DBTDL are added. The mixture reacts for 3 h at 450 rpm, keeping the temperature constant during this step. After this time, temperature is lowered to 40 °C before adding the required acetone. The mixture is left to stir for a further hour before adding TEA to neutralize the acidic groups coming from DMPA. This step takes 30 min to reach the complete neutralization of

Table 1 WBPUR aerogels synthesis conditions

DMPA/NMP ($\text{mol}\cdot\text{mol}^{-1}$)	Acetone/PUR ($\text{wt}\cdot\text{wt}^{-1}$)	TEA/DMPA ($\text{mol}\cdot\text{mol}^{-1}$)	EDA/HMDI ($\text{mol}\cdot\text{mol}^{-1}$)	NCO/OH ($\text{mol}\cdot\text{mol}^{-1}$)	DBTDL/PEG ($\text{wt}\cdot\text{wt}^{-1}$)
1	1.25	1.2	0.33	1.5	0.5

carboxylic groups. All the above steps were carried out under a stream of N₂ to create an inert atmosphere. The next step is to add EDA in excess to the mixture, which will elongate the polymer chains giving another 30 min to the process. The last stage of the synthesis process is reached by adding water and dispersing the polymer. The amount of water added depends on the desired solid content for the final aerogel.

Once the mixture is completely dispersed in water, the dispersion is transferred to steel trays, where it will be aged for 1 day at 25 °C before being introduced in the freeze-dryer. Finally, a freeze-drying cycle with some different stages (congelation, primary and secondary drying) is launched, which will eliminate the water from the mixture by sublimation, thus generating the final aerogel. Specifically, the conditions employed in this process are freezing for 5.5 h at – 40 °C, subsequently a primary drying is carried out for 60 h at 25 °C and 200 μbar and, finally, a secondary drying for 10 h at 40 °C. The cooling or heating ramps required during the freeze-drying process have a duration of 1 h.

Characterization techniques

The *bulk density* of materials was determined by using an electronic scale (PCE-LS, PCE Instruments). The methodology followed is based over the Archimedes principle: the density is calculated comparing the mass of the material measured in both air and water and considering the density of the water used as fluid [39].

Thermal conductivities of the aerogels were measured using a Heat Flow Meter (KD2Pro, Decagon Devices Inc.). The KS-1 Sensor (a 6 cm long skewer) was introduced in the material and the equipment shows the thermal conductivity of the given material on screen, in a range from 0.02 to 2.00 W m⁻¹ K⁻¹. Sample dimensions used were 30 × 30 × 2 cm (width × length × thickness), and an average of at least three measurements was taken to report.

Chemical structure of the samples was studied using an infrared spectrometer (Spectrum Two, PerkinElmer) in the range of 500–4000 cm⁻¹.

The *morphological structure* was analysed using a scanning electron microscopy (SEM, Model Phenom-ProX, Phenom World).

The *Young's modulus* was determined using dynamic mechanical analysis (DMA, 1STARe System,

Mettler Toledo) by means of stress–strains analyses in compression mode. Samples used to perform these analyses were of ca. 1 × 1 × 0.6 cm (width × length × thickness) dimensions. An average of at least three measurements was taken to report.

Thermogravimetric analysis (TGA) using a thermal analyser (TGA, 2STARe System, Mettler Toledo) was carried out to evaluate the *thermal stability* of the produced aerogels. Furthermore, the glass transition temperature was determined on a differential scanning calorimetry (DSC, 2STARe System, Mettler Toledo) using a heating rate of 20 K min⁻¹ from – 80 to 100 °C.

Contact angles were measured using an optical tensiometer at 25 °C (Theta Lite, Biolin Scientific). For that, two microlitres of water were dropped onto the surface of polyurethane aerogels. The average contact angle was obtained by measuring the real contact angle between the drop and the sample at two different positions.

Results and discussion

Study of feasibility of the developed WBPUR synthesis process

To check the feasibility of the proposed synthesis process, the physicochemical characteristics of the baseline WBPUR aerogel were thoroughly evaluated. It should be noted that during the synthesis process, it is of great importance to avoid hydration of the reagents, as the isocyanate groups can react with the water maybe present in the reagents as traces. Preliminary experiments were performed using the synthesis procedure described in Fig. 1. It is important to note that, until a successful synthesis

Table 2 Quantity of reagents used to synthesize the baseline WBPUR aerogel

Reagent	Quantity
HMDI (mL)	24.3
PEG (g)	32.9
DMPA (g)	6.6
TEA (mL)	8.2
EDA (mL)	2.2
NMP (mL)	4.8
Acetone (mL)	116.1
DBTDL (mL)	0.2
Water (mL)	904.8

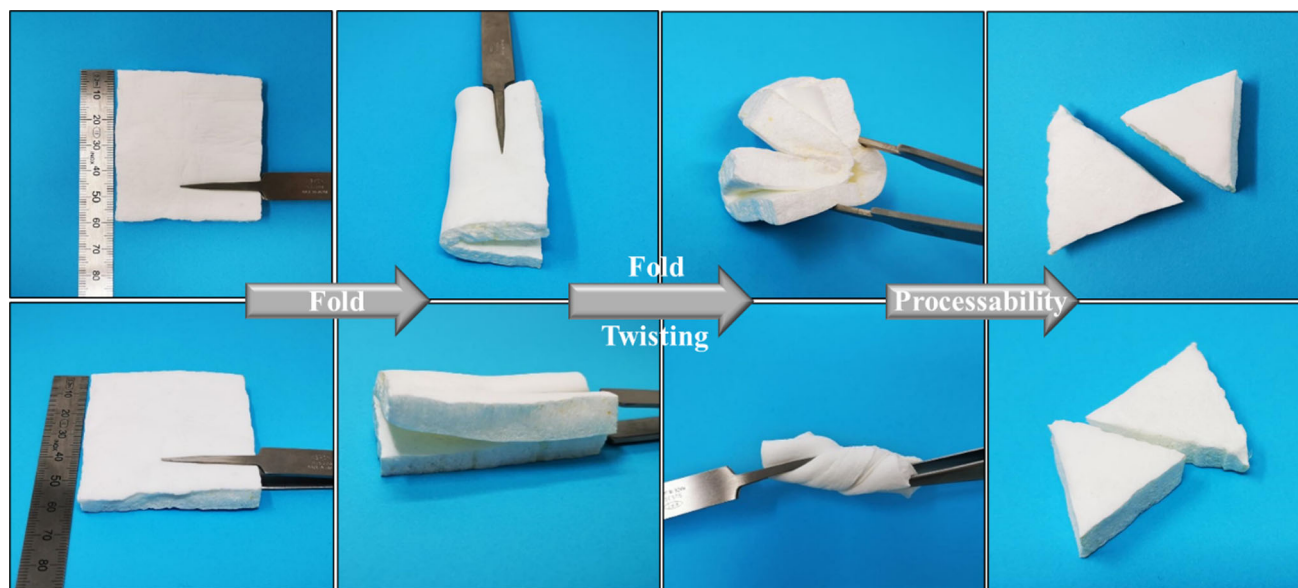


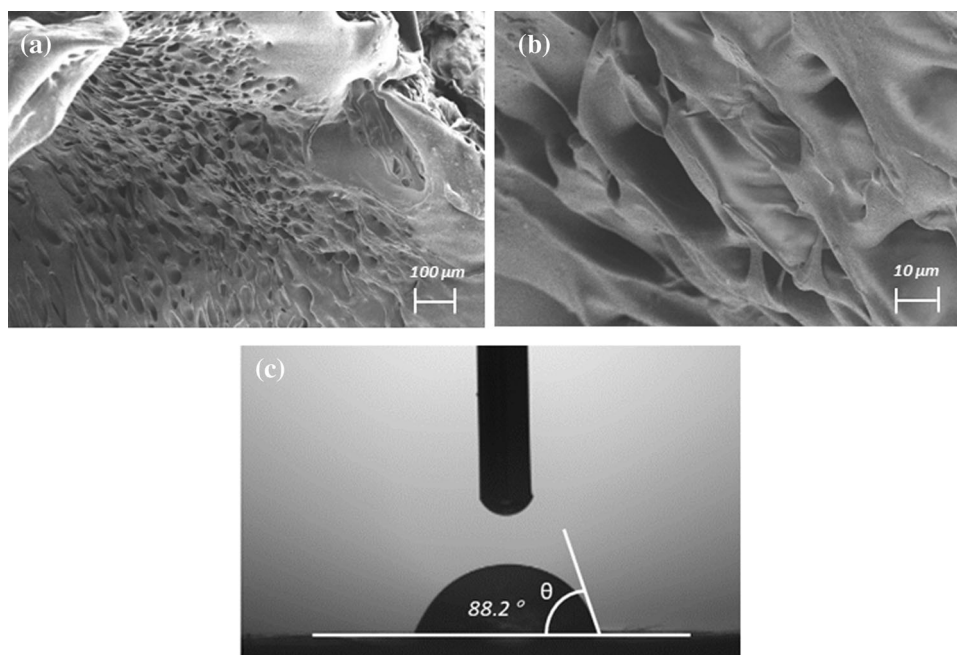
Figure 2 Physical appearance of the baseline WBPUR aerogel.

procedure was obtained with an aerogel of suitable properties, multiple tests were carried out varying different parameters (not shown in this work). The quantities of each reagent finally used are shown in Table 2. Note that water content was adjusted so that the solids content was 7.5%. Once the recipe explained above had been experimentally carried out, WBPUR aerogels were obtained, their visual appearance can be seen in Fig. 2. As observed, WBPUR aerogels obtained turned out to be robust

and highly resistant to being fold several times and even twisted. Its handling and easy modelling in particular forms demonstrate the great processability of this material. These mechanical properties are similar to that obtained from other authors (high bendability and elasticity) [40, 41].

The morphology of synthesized WBPUR aerogel was evaluated by means of SEM (Fig. 3a, b). SEM micrographs displayed a porous network microstructure, which was mainly achieved

Figure 3 a, b SEM micrographs at two different scales and c contact angle of the baseline WBPUR aerogel.



throughout the sublimation of water during freeze-drying process. During the freeze-drying, the solvent molecules entrapped between the polymer molecular chains are gradually sublimated, creating a microporous structure which could give the material insulating properties [42, 43]. It can be observed in more detail the microchannels created in Fig. 3b. The contact angle depends on different issues and generally enhances with increasing hydrophobicity, surface roughness crosslink density and glass transition temperature of the surface [44]. As shown in Fig. 3c, the average contact angle of the baseline aerogel was 88.2 ± 1.0 °C ($n = 2$), less than 90 °C, indicating the hydrophilic character of the obtained material [45].

Fourier-transform infrared spectroscopy (FT-IR) analysis of reference sample is showed in Fig. 4. In the spectrum, the band located at 1710 cm^{-1} is associated with the stretching vibration of urethane and allophanate groups, while bands located at $3040\text{--}2760\text{ cm}^{-1}$ are assigned to the stretching vibrations of C-H from alkanes [5, 46]. In view of these results, the absence of absorption peaks at $2470\text{--}2025\text{ cm}^{-1}$ region corresponds to stretching vibrations of N=C=O functionalities (isocyanate), indicating the complete reaction of the isocyanate at the end of the synthesis process. Thus, it is demonstrated the formation of the polyurethane, as well as

the elongation of the polymer chains before the freeze drying.

DSC analyses were performed to examine the crystalline phases in the PUR structure that are formed by the hard and soft segments [47]. DSC curves from the first and second heating scans of WBPUR aerogel are shown in Fig. 5. These heating profiles show the glass transition (T_g) of the soft segments at approximately -50 °C and another slight relaxation transition is observed at 55 °C corresponding to hard segments [48].

Finally, thermal stability of the baseline aerogel was tested by TGA analysis under an inert nitrogen atmosphere. Figure 6 shows the pyrolysis process alongside the derivative of the weight with respect to the temperature. This sample exhibited three decomposition stages. The first stage, which occurred in the range $25\text{--}230$ °C, corresponds to the evaporation of residual solvents such as NMP and the remaining adsorbed water [49]. The second stage, which appeared in the range $230\text{--}440$ °C can be assigned to the thermal decomposition process of the main chains of polyurethane molecules [50]. Around 15 wt. % remained at the end of this stage. Finally, the third stage, which ranged $440\text{--}650$ °C, indicated a maximum weight loss of approximately 99% due to the decomposition of ester groups [51, 52]. At the end

Figure 4 FT-IR spectra of HMDI and the baseline WBPUR aerogel.

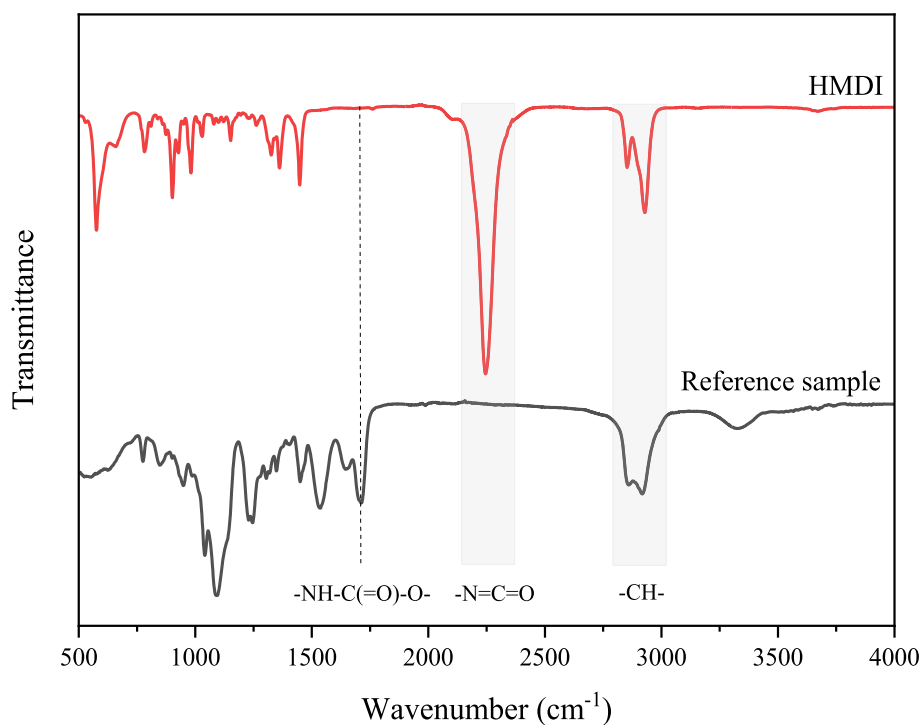


Figure 5 DSC curve of the obtained WBPUR aerogel.

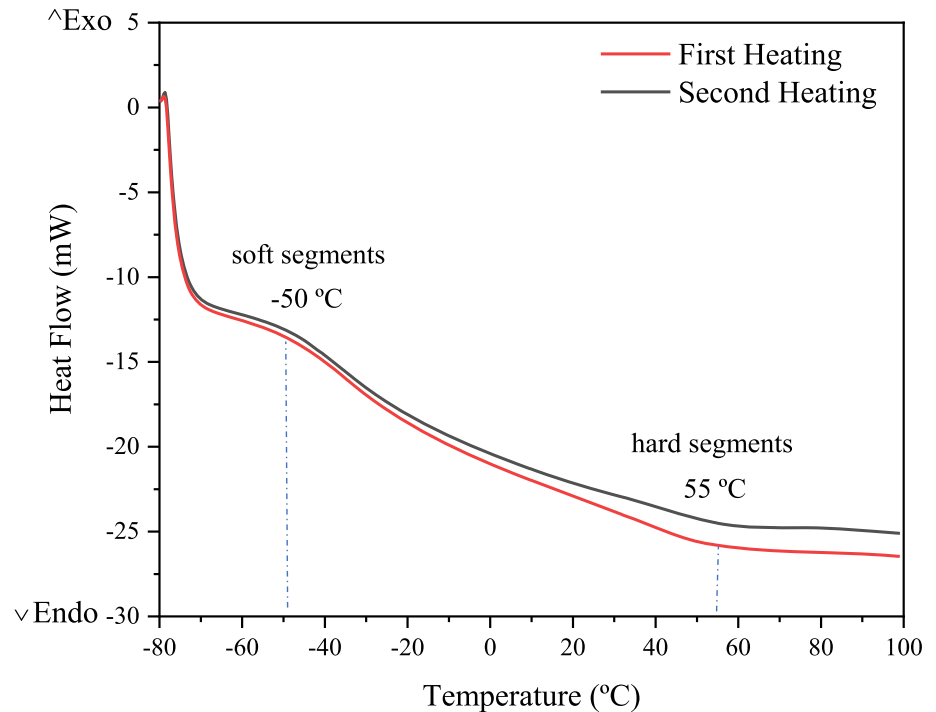
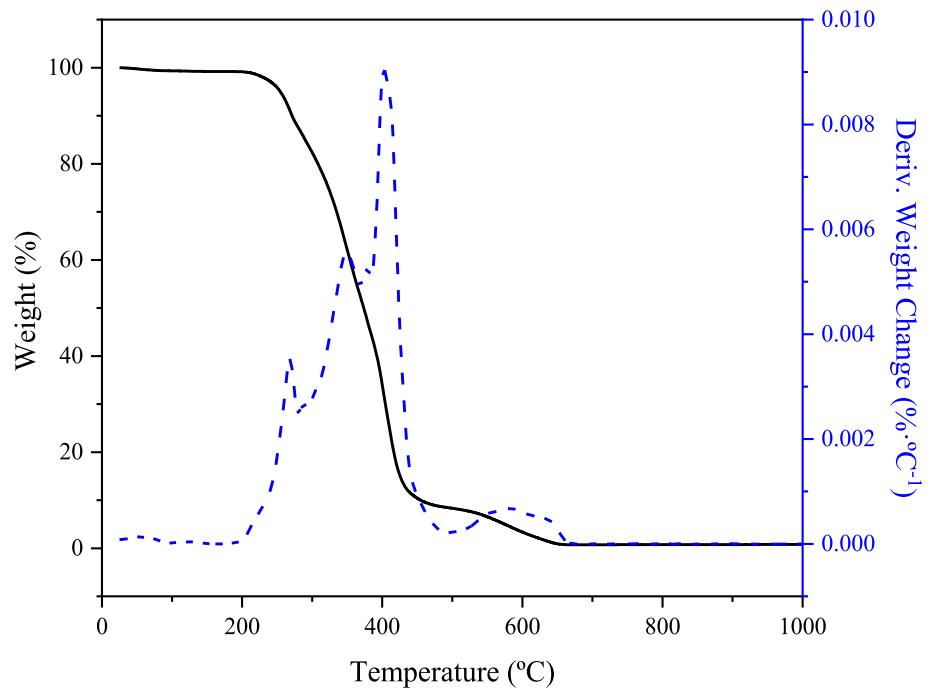


Figure 6 TGA (black solid line) and DTGA (blue dotted line) curves of the baseline WBPUR aerogel.



of this stage, 0.87 wt. % of the sample remained at 1000 °C. Thus, it can be confirmed that this material is thermally stable up to 230 °C, temperature at which the degradation of the polymeric network starts.

Influence of solids content (wt.·wt.⁻¹)

Since the main application of the developed aerogels is to act as thermal insulators mainly in the exterior walls of buildings, both density and thermal conductivity of these materials must be as low as possible, while maintaining their mechanical properties. In

this sense, the amount of solids dispersed in water (solids content (wt.·wt.⁻¹)) used to obtain the PUR hydrogel was modified from 2 to 15% to evaluate the mentioned properties in the final WBPUR aerogels. The quantities of each reagent to prepared WBPUR aerogels with different solids content are summarized in Table S1. Solids content (wt.·wt.⁻¹) relation was calculated as shown in Eq. (1):

$$\text{Solids content (wt. · wt.⁻¹)} = \frac{\sum_{\text{weight}} (\text{HMDI} + \text{PEG} + \text{DMPA} + \text{TEA} + \text{EDA})}{\sum_{\text{weight}} (\text{HMDI} + \text{PEG} + \text{DMPA} + \text{TEA} + \text{EDA} + \text{water})} \quad (1)$$

Thus, solids content of the aerogels is calculated with respect to the total amount of reactants that participate in the formation of the polymer (PEG, HMDI, DMPA, TEA and EDA), excluding the reagents acetone, NMP and DBTDL.

The morphology of the materials can be predicted from the SEM micrographs. The porous structure of

the different obtained aerogels depending on the solid content can be shown in Fig. 7. Herein, the porous amount clearly decreases with higher solids content. Thus, different packing was observed as a function of porosity, resulting in the observed changes in density values as detailed below. It can be observed that, as such content decreases, there is a more porous structure, while at higher contents, between 10 and 15%, the structure of the aerogels is practically non-porous, thus, being a much rigid and less flexible material. On the other hand, a low solid content is associated with very soft and brittle materials that may even deformed.

Density and thermal conductivity values of synthesized WBPUR aerogels are shown in Fig. 8 and Table S1. A priori, aerogels synthesized using 2 and 15% of solid content were discarded due to the first one is brittle and very weak, and the latter is just the opposite. Therefore, they were not suitable for final application. As expected, the density of the obtained

Figure 7 SEM micrographs of the prepared WBPUR aerogels obtained using different solids contents **a** 2%, **b** 2.5%, **c** 5%, **d** 7.5% **e** 10% and **f** 15%.

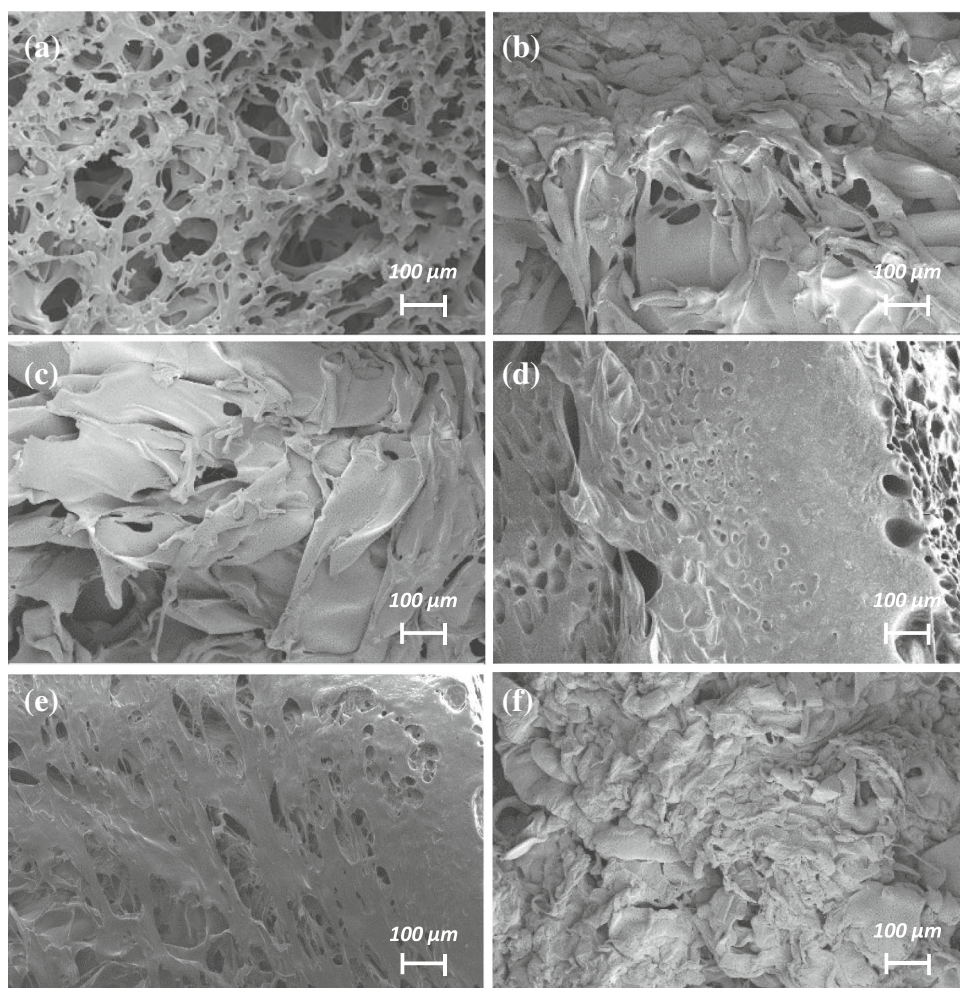
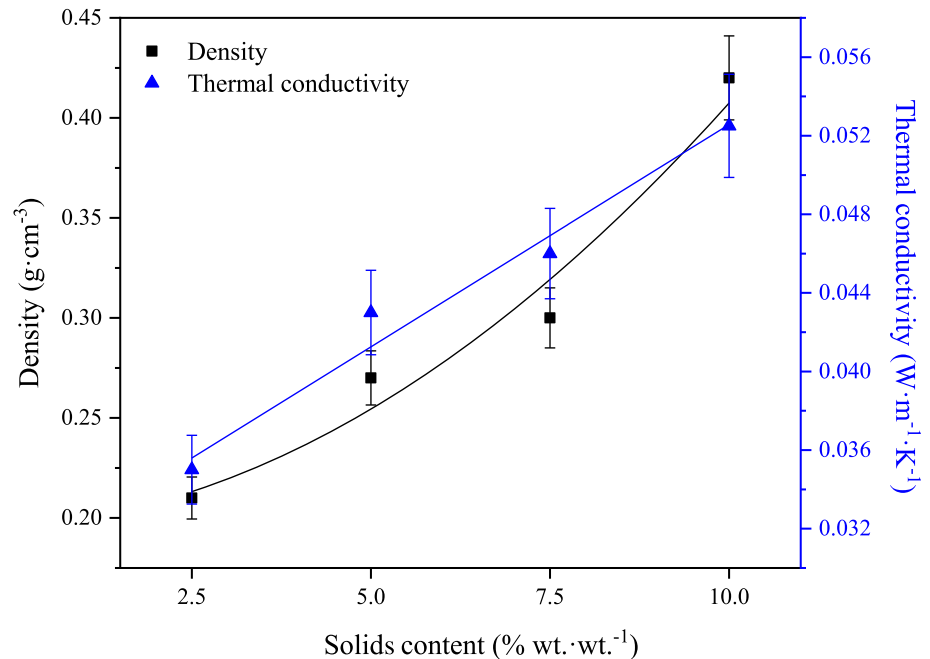


Figure 8 Density and thermal conductivity of WBPUR aerogels obtained using different % solids content.

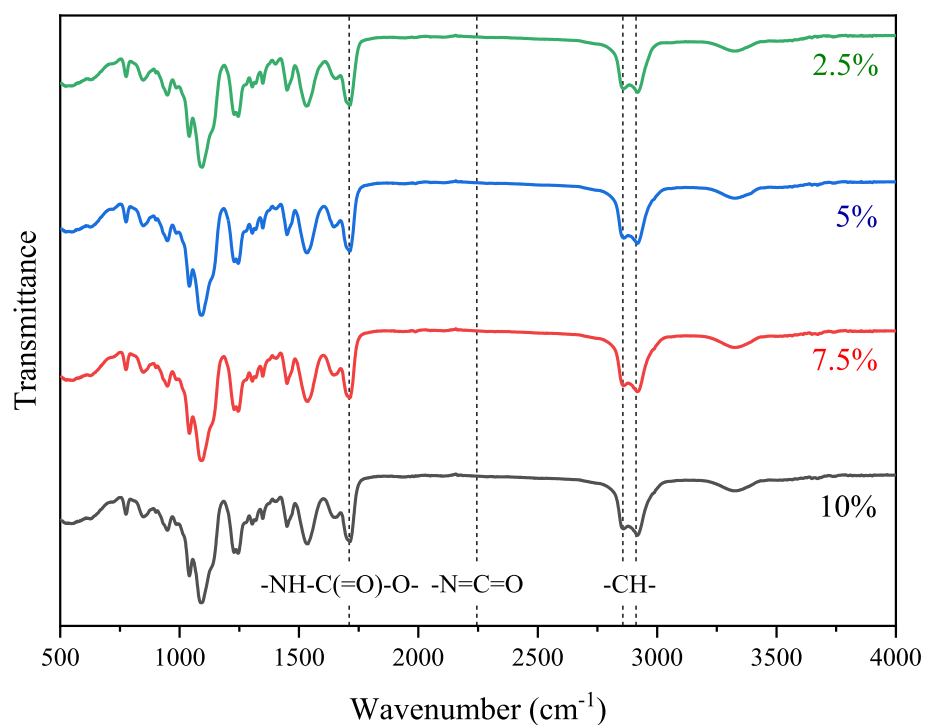


aerogels increased with the solid content of the sample, and so does the thermal conductivity. As previously observed, this increase in density with higher solids content leads to a noticeable reduction in the pore quantity, contributing to an increase in heat transfer [4]. Therefore, in view of these results, it can be confirmed that a higher porosity in the synthesized aerogels structures is associated with a

lower thermal conductivity, thus favouring its capacity as a thermal insulator.

As previously, the correct formation of the polyurethane was verified by FT-IR. All the samples presented similar curves (Fig. 9), in which the absence of a peak in the wavelength associated with the $-N=C=O$ group ($2470\text{--}2025\text{ cm}^{-1}$) and the presence of the band associated with the stretching

Figure 9 FT-IR profiles of WBPUR aerogels obtained using different % solids content.



vibration of urethane and allophanate groups appearing at 1710 cm^{-1} , confirm the correct formation of the polyurethane after the synthesis and the correct elongation of the polymeric chains before the freeze-drying process.

To analyse the influence of the solids content on the thermal stability of the final aerogel, TGA analyses were performed on all valid samples showing the results obtained in Fig. 10. All samples showed a similar pattern, maintaining the thermal degradation zones previously commented (Fig. 6), being all of them stable up to $230\text{ }^{\circ}\text{C}$. Again, all synthesized WBPUR aerogels showed three thermal degradation stages: evaporation of solvents ($25\text{--}230\text{ }^{\circ}\text{C}$), decomposition of polyurethane chains ($230\text{--}440\text{ }^{\circ}\text{C}$), and degradation of ester groups ($440\text{--}650\text{ }^{\circ}\text{C}$), with similar weight loss to the ones perceived with reference sample. As all samples showed similar TGA and DTGA behaviours, and based on the FT-IR results, the correct formation of polyurethane can be confirmed for all synthesized samples.

Additionally, to check the mechanical behaviour of the synthesized aerogels and to correlate it with their physical properties, dynamic mechanical analyses (DMA) were performed to the samples. These experiments were carried out by following a stress–strain method, carried out at a constant temperature of $25\text{ }^{\circ}\text{C}$. Figure 11 presents typical stress–strain

curves for the aerogels obtained using the already mentioned solid contents. Each curve represents the experienced strain when small stresses (from 0 to 2 N) are applied. Although these curves could reveal many properties of a material, these studies were carried out by focusing on the Young's modulus of each sample, determined by the slope of the linear part of the stress–strains curve, where an elastic behaviour was observed (Table S1). As observed, solid content has a marked effect on the mechanical properties of polyurethane aerogels, with the slope of the curves increasing with the amount of solid content dispersed in water during the synthesis process [53]. Consequently, Young's modulus experiences a marked increase from 0.005 to 0.136 MPa (Table S1), demonstrating the loss of mechanical capabilities and stiffness of materials as their density and thermal conductivity decrease. In addition, Fig. 11b shows the power-law correlation between the elastic modulus of the WBPUR aerogels with their density. As can be seen, the elastic Young's modulus (E) strongly increases with the density (ρ) and this evolution follows a power law such as $E \propto \rho^{3.6}$. This trend agrees with the literature values [54, 55].

Figure 10 TGA (solid lines) and DTGA (dotted lines) curves of WBPUR aerogels obtained using different % solids content.

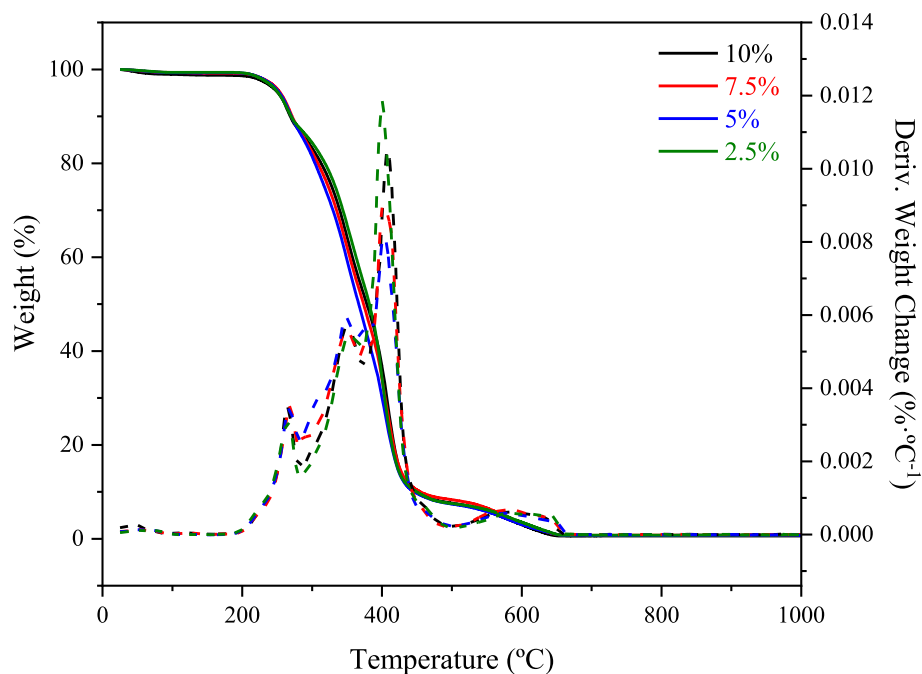
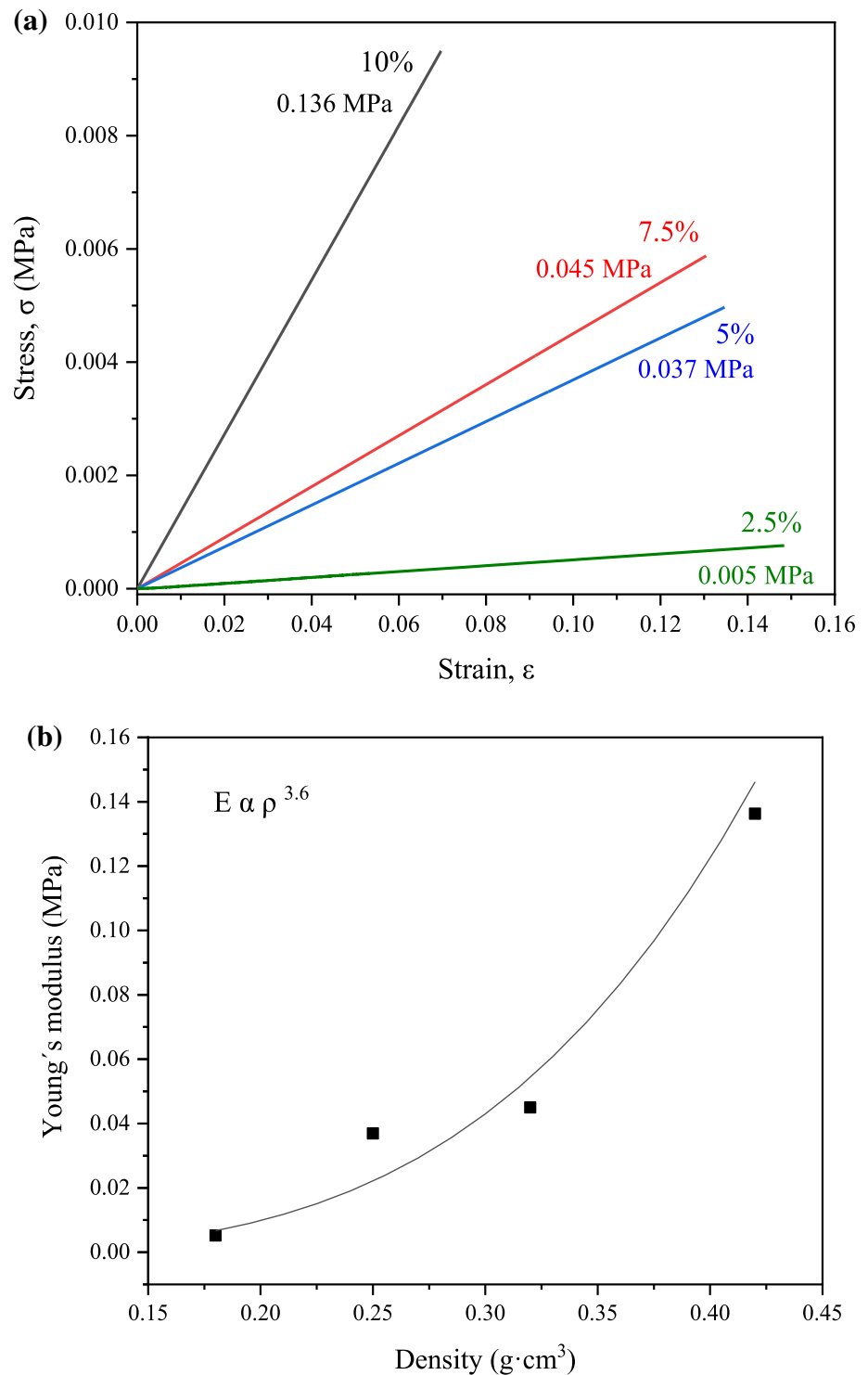


Figure 11 **a** Compressive stress–strain curves and **b** relationship between the Young’s modulus vs density for WBPUR aerogels obtained using different % solids content.



Conclusions

WBPUR aerogels were successfully prepared via a stepwise polymerization process followed by freeze-drying method. The important dependence of the solids content of this type of materials on their

physical properties can be highlighted. Depending on this consideration, the porous materials obtained have a density between 0.21 and 0.42 $\text{g}\cdot\text{cm}^{-3}$, thermal conductivity between 0.035 and 0.052 $\text{W}\cdot\text{m}^{-1}\cdot\text{K}^{-1}$ and Young's modulus between 0.005 and 0.136 MPa when using between 2.5 and 10% solids content,

respectively. As these are light and insulating materials, the ideal sample for this application will be the one containing 2.5% of solids present in the aerogel structure. Based on these preliminary results, a promising new route is proposed as a simple, efficient, and low-cost alternative to the existing ones.

Acknowledgements

This present work was performed within the framework of the BIOMAT project. This project has received funding from the European Union's Horizon 2020 research and innovation programme under Grant Agreement No. 953270.

Author's contribution

DC was involved in investigation, methodology and writing—original draft preparation; EPP contributed to formal analysis, visualization, data curation and editing; AR was involved in conceptualization, methodology, writing—review and supervision. LSS contributed to conceptualization, writing—review, supervision, project administration and funding acquisition.

Funding

Open Access funding provided thanks to the CRUE-CSIC agreement with Springer Nature.

Declarations

Conflict of interest The authors declare no conflicts of interests.

Ethical approval Not applicable.

Supplementary information A brief description of the additional material omitted from the main body is accompanied in order to present a clearer and more readable manuscript.

Supplementary Information: The online version contains supplementary material available at <http://doi.org/10.1007/s10853-023-08579-0>.

Open Access This article is licensed under a Creative Commons Attribution 4.0 International

License, which permits use, sharing, adaptation, distribution and reproduction in any medium or format, as long as you give appropriate credit to the original author(s) and the source, provide a link to the Creative Commons licence, and indicate if changes were made. The images or other third party material in this article are included in the article's Creative Commons licence, unless indicated otherwise in a credit line to the material. If material is not included in the article's Creative Commons licence and your intended use is not permitted by statutory regulation or exceeds the permitted use, you will need to obtain permission directly from the copyright holder. To view a copy of this licence, visit <http://creativecommons.org/licenses/by/4.0/>.

References

- [1] Adhikary SK, Ashish DK, Rudžionis Ž (2021) Aerogel based thermal insulating cementitious composites: a review. *Energy Build* 245:111058–111082. <https://doi.org/10.1016/j.enbuild.2021.111058>
- [2] Li Y, Yang L, He B, Zhao D (2014) Green building in China: needs great promotion. *Sustain Cities Soc* 11:1–6. <https://doi.org/10.1016/j.scs.2013.10.002>
- [3] Członka S, Bertino MF, Kośny J, Shukla N (2020) Density and shrinkage as guiding criteria for the optimization of the thermal conductivity of poly(urethane)-class aerogels. *J Sol-gel Sci Technol* 93:149–167. <https://doi.org/10.1007/s10971-019-05161-6>
- [4] Członka S, Bertino MF, Kośny J, Shukla N (2018) Freeze-drying method as a new approach to the synthesis of polyurea aerogels from isocyanate and water. *J Sol-gel Sci Technol* 87:685–695. <https://doi.org/10.1007/s10971-018-4769-9>
- [5] Simón-Herrero C, Chen XY, Ortiz ML, Romero A, Valverde JL, Sánchez-Silva L (2019) Linear and crosslinked polyimide aerogels: Synthesis and characterization. *J Mater Res Technol* 8:2638–2648. <https://doi.org/10.1016/j.jmrt.2019.02.016>
- [6] Zhu Z, Snellings GMBF, Koebel MM, Malfait WJ (2017) Superinsulating polyisocyanate based aerogels: a targeted search for the optimum solvent system. *ACS Appl Mater Interfaces* 9:18222–18230. <https://doi.org/10.1021/acsami.7b03344>
- [7] Merillas B, Villafaña F, Rodríguez-Pérez MÁ (2022) Superinsulating transparent polyisocyanurate-polyurethane aerogels: analysis of thermal conductivity and mechanical

- properties. *Nanomaterials* 12:2409–2426. <https://doi.org/10.3390/nano12142409>
- [8] Casini M (2014) Smart materials and nanotechnology for energy retrofit of historic buildings. *Int J Civ Eng* 1:28–37. <https://doi.org/10.15224/978-1-63248-020-0-18>
- [9] Cuce E, Cuce PM, Wood CJ, Riffat SB (2014) Toward aerogel based thermal superinsulation in buildings: A comprehensive review. *Renew Sust Energ Rev* 34:273–299. <https://doi.org/10.1016/j.rser.2014.03.017>
- [10] Koebel M, Rigacci A, Achard P (2012) Aerogel-based thermal superinsulation: An overview. *J Solgel Sci Technol* 63:315–339. <https://doi.org/10.1007/s10971-012-2792-9>
- [11] Ricci A, Bernardi L, Gioia C, Vierucci S, Robitzer M, Quignard F (2010) Chitosan aerogel: a recyclable, heterogeneous organocatalyst for the asymmetric direct aldol reaction in water. *Chem Comm* 46:6288–6290. <https://doi.org/10.1039/c0cc01502d>
- [12] Liu W, Herrmann AK, Bigall NC et al (2015) Noble metal aerogels-synthesis, characterization, and application as electrocatalysts. *Acc Chem Res* 48:154–162. <https://doi.org/10.1021/ar500237c>
- [13] Leventis N (2022) Polyurea aerogels: Synthesis, material properties, and applications. *Polymers* 14:969–1015. <https://doi.org/10.3390/polym14050969>
- [14] Efthalia G, Pashalidis I, Raptopoulos G, Paraskevopoulou P (2022) Efficient removal of polyvalent metal ions (Eu(III) and Th(IV)) from aqueous solutions by polyurea-crosslinked alginate aerogels. *Gels* 8:478–489. <https://doi.org/10.3390/gels8080478>
- [15] Soleimani Dorcheh A, Abbasi MH (2008) Silica aerogel; synthesis, properties and characterization. *J Mater Process Technol* 199:10–26. <https://doi.org/10.1016/j.jmatprotec.2007.10.060>
- [16] Gurav JL, Jung IK, Park HH, Kang ES, Nadargi DY (2010) Silica aerogel: Synthesis and applications. *J Nanomater* 2010:1–11. <https://doi.org/10.1155/2010/409310>
- [17] Thomas S, Datta J, Haponiuk JT, Reghunadhan A (2017) *Polyurethane polymers: composites and nanocomposites*, 1st edn. Elsevier, Chennai
- [18] Abdul Khalil HPS, Bashir Yahya E, Jummaat F, Adnan AS, Olaiya NG, Rizal S, Abdullah CK, Pasquini D, Thomas S (2023) Biopolymers based aerogels: a review on revolutionary solutions for smart therapeutics delivery. *Prog Mater Sci* 131:101014–101048. <https://doi.org/10.1016/j.pmatsci.2022.101014>
- [19] Merillas B, Martín-de León J, Villafane F, Rodríguez-Pérez MA (2021) Transparent polyisocyanurate-polyurethane-based aerogels: key aspects on the synthesis and their porous structures. *ACS Appl Polym Mater* 3:4607–4615. <https://doi.org/10.1021/acsapm.1c00712>
- [20] Aney S, Schettler J, Schwan M, Milow B, Rege A (2022) Insights into the micromechanics of organic aerogels based on experimental and modeling results. *Adv Eng Mater* 24:1–8. <https://doi.org/10.1002/adem.202100095>
- [21] Moreno-Castilla C, Maldonado-Hódar FJ (2005) Carbon aerogels for catalysis applications: An overview. *Carbon* 43:455–465. <https://doi.org/10.1016/j.carbon.2004.10.022>
- [22] Liu Z, Ran Y, Xi J, Wang J (2020) Polymeric hybrid aerogels and their biomedical applications. *Soft Matter* 16:9160–9175. <https://doi.org/10.1039/d0sm01261k>
- [23] Tan C, Fung BM, Newman JK, Vu C (2001) Organic aerogels with very high impact strength. *Adv Mater* 13:644–646. [https://doi.org/10.1002/1521-4095\(200105\)13:9%3c644::aid-adma644%3e3.0.co;2-%23](https://doi.org/10.1002/1521-4095(200105)13:9%3c644::aid-adma644%3e3.0.co;2-%23)
- [24] Feng J, Wang X, Tian Y, Luo C, Sun M (2018) Melamine-formaldehyde aerogel coating for in-tube solid-phase microextraction. *J Chromatogr A* 1577:8–14. <https://doi.org/10.1016/j.chroma.2018.09.047>
- [25] Diascorn N, Calas S, Sallée H, Achard P, Rigacci A (2015) Polyurethane aerogels synthesis for thermal insulation—textural, thermal and mechanical properties. *J Supercrit Fluids* 106:76–84. <https://doi.org/10.1016/j.supflu.2015.05.012>
- [26] Biesmans G, Mertens A, Duffours L, Woignier T, Phalippou J (1998) Polyurethane based organic aerogels and their transformation into carbon aerogels. *J Non Cryst Solids* 225:64–68. [https://doi.org/10.1016/S0022-3093\(98\)00010-6](https://doi.org/10.1016/S0022-3093(98)00010-6)
- [27] Yoo HJ, Do KH (2008) Synthesis and properties of waterborne polyurethane hydrogels for wound healing dressings. *J Biomed Mater Res B Appl Biomater* 85:326–333. <https://doi.org/10.1002/jbm.b.30950>
- [28] Teymouri M, Kokabi M, Alamdarnejad G (2020) Conductive shape-memory polyurethane/multiwall carbon nanotube nanocomposite aerogels. *J Appl Polym Sci* 137:1–11. <https://doi.org/10.1002/app.48602>
- [29] Levy D, Zayat M (2015) *The Sol–Gel Handbook*, 1st edn. Wiley-VCH, Weinheim
- [30] He R, Xie C, Chen Y, Guo Z-X, Guo B, Tuo X (2022) Robust and highly resilient waterborne polyurethane-based composite aerogels prepared by blending with aramid nanofibers. *Compos Sci Technol* 228:109622. <https://doi.org/10.1016/j.compscitech.2022.109622>
- [31] Aegerter MA, Leventis N, Koebel MM (2011) *Aerogels Handbook*, 1st edn. Springer, New York
- [32] Meng L, Shi X, Zhang R, Yan L, Liang Z, Nie Y, Zhou Z, Hao T (2020) Preparation and properties study of waterborne polyurethane synthesized by mixing polyester diols and isocyanates. *J Appl Polym Sci* 137:49314. <https://doi.org/10.1002/app.49314>

- [33] Honarkar H (2018) Waterborne polyurethanes: a review. *J Dispers Sci Technol* 39:507–516. <https://doi.org/10.1080/01932691.2017.1327818>
- [34] Cakić SM, Ristić IS, Ristić OZ (2012) Thermal Analysis of Polyurethane Dispersions Based on Different Polyols. In: Zafar F, Sharmin E (eds) *Polyurethane*. InTechOpen, New Delhi, pp 79–100
- [35] Vareda JP, Lamy-Mendes A, Durães L (2018) A reconsideration on the definition of the term aerogel based on current drying trends. *Microporous Mesoporous Mater* 258:211–216. <https://doi.org/10.1016/j.micromeso.2017.09.016>
- [36] Chidambareswarapattar C, McCarver PM, Luo H, Lu H, Sotiriou-Leventis C, Leventis N (2013) Fractal multiscale nanoporous polyurethanes: flexible to extremely rigid aerogels from multifunctional small molecules. *Chem Mater* 25:3205–3224. <https://doi.org/10.1021/cm401623h>
- [37] Cheikh W, Rózsa ZB, Camacho CO, Mizsey P, Viskolcz B, Szőri M, Fejes Z (2019) Urethane formation with an excess of isocyanate or alcohol: experimental and Ab initio study. *Polymers* 11:1543–1553. <https://doi.org/10.3390/polym11101543>
- [38] Asociación Española de Normalización y Certificación (AENOR) UNE-EN 1242:2013: Adhesives. Determination of isocyanate content
- [39] Mohazzabi P (2017) Archimedes' principle revisited. *J Appl Math Phys* 5:836–843. <https://doi.org/10.4236/jamp.2017.54073>
- [40] Bang A, Buback C, Sotiriou-Leventis C, Leventis N (2014) Flexible aerogels from hyperbranched polyurethanes: probing the role of molecular rigidity with poly (urethane acrylates) versus poly (urethane norbornenes). *Chem Mater* 26:6979–6993. <https://doi.org/10.1021/cm5031443>
- [41] Donthula S, Mandal C, Leventis T, Schisler J, Saeed AM, Sotiriou-Leventis C, Leventis N (2017) Shape memory superelastic poly (isocyanurate-urethane) aerogels (PIR-PUR) for deployable panels and biomimetic applications. *Chem Mater* 29:4461–4477. <https://doi.org/10.1021/acs.chemmater.7b01020>
- [42] Qiang T, Wang S, Wang Z, Ren L (2022) Recyclable 3D Konjac glucomannan/graphene oxide aerogel loaded with ZIF-67 for comprehensive adsorption of methylene blue and methyl orange. *J Ind Eng Chem* 116:371–384. <https://doi.org/10.1016/j.jiec.2022.09.027>
- [43] Wang J, Yi D, Peng X, Yang H, Wang T, Gao J, Xie B, Su G (2022) The hydrophobically modified cellulose-based aerogel loaded with BTA enhances the anticorrosion and active self-healing properties of epoxy coating. *Colloids Surf A Physicochem Eng Asp* 653:129835–129846. <https://doi.org/10.1016/j.colsurfa.2022.129835>
- [44] Kim HA, Kim BK (2019) Synthesis and properties of waterborne polyurethane/hydroxyapatite chemical hybrids. *Prog Org Coat* 128:69–74. <https://doi.org/10.1016/j.porgcoat.2018.12.009>
- [45] Kwok DY, Neumann AW (1999) Contact angle measurement and contact angle interpretation. *Adv Colloid Interface Sci* 81:167–249. [https://doi.org/10.1016/S0001-8686\(98\)00087-6](https://doi.org/10.1016/S0001-8686(98)00087-6)
- [46] Xu L, Liu Y, Xin B, Zhou Y (2022) Preparation and properties of functional fabric coating based on SiO₂-aerogel/polyurethane. *Fibers Polym* 23:1870–1880. <https://doi.org/10.1007/s12221-022-4675-1>
- [47] Cao Z, Zhou Q, Jie S, Li BG (2016) High cis-1,4 hydroxyl-terminated polybutadiene-based polyurethanes with extremely low glass transition temperature and excellent mechanical properties. *Ind Eng Chem Res* 55:1582–1589. <https://doi.org/10.1021/acs.iecr.5b04921>
- [48] Somdee P, Lassú-Kuknyó T, Kónya C, Szabó T, Marossy K (2019) Thermal analysis of polyurethane elastomers matrix with different chain extender contents for thermal conductive application. *J Therm Anal Calorim* 138:1003–1010. <https://doi.org/10.1007/s10973-019-08183-y>
- [49] Zhang XM, Liu JG, Yang SY (2016) Synthesis and characterization of flexible and high-temperature resistant polyimide aerogel with ultra-low dielectric constant. *Exp Polym Lett* 10:789–798. <https://doi.org/10.3144/expresspolymlett.2016.74>
- [50] Cobos M, Pagalday E, Puyadena M, Cabido X, Martín L, Múgica A, Irusta L, González A (2023) Waterborne hybrid polyurethane coatings containing casein as sustainable green flame retardant through different synthesis approaches. *Prog Org Coat* 174:107278–107296. <https://doi.org/10.1016/j.porgcoat.2022.107278>
- [51] Trovati G, Sanches EA, Neto SC, Mascarenhas YP, Chierice GO (2010) Characterization of polyurethane resins by FTIR, TGA, and XRD. *J Appl Polym Sci* 115:263–268
- [52] Claro CJM, Neto S, Chierice GO, Santos AM (2006) Study of the biodegradation of a polymer derived from castor oil by scanning electron microscopy, thermogravimetry and infrared spectroscopy. *Polímeros* 16:129–135
- [53] Simón-Herrero C, Romero A, Valverde JL, Sánchez-Silva L (2018) Hydroxyethyl cellulose/alumina-based aerogels as lightweight insulating materials with high mechanical strength. *J Mater Sci* 53:1556–1567. <https://doi.org/10.1007/s10853-017-1584-6>
- [54] Ma H, Zheng X, Luo X, Yi Y, Yang F (2018) Simulation and analysis of mechanical properties of silica aerogels: From

rationalization to prediction. *Materials* 11:214–225. <https://doi.org/10.3390/ma11020214>

- [55] Woignier T, Primera J, Alaoui A, Despetis F, Calas-Etienne S, Faivre A, Duffours L, Levelut C, Etienne P (2020) Techniques for characterizing the mechanical properties of

aerogels. *J Solgel Sci Technol* 93:6–27. <https://doi.org/10.1007/s10971-019-05173-2>

Publisher's Note Springer Nature remains neutral with regard to jurisdictional claims in published maps and institutional affiliations.